ONLINE FIRST

ISSN: 0015-5659

e-ISSN: 1644-3284

Reconstruction of lymphatic vessels in the mouse tail after cupping therapy

Authors: Fanwei Meng, Zhan-Ling Gao, Li Li, Lin-Lin Jie, Peng-Fei Yang, Zheng Liang, Ya-Wei Gao, Wen-Hui Liu

DOI: 10.5603/FM.a2019.0044

Article type: ORIGINAL ARTICLES

Submitted: 2019-03-13

Accepted: 2019-04-07

Published online: 2019-04-11

Reconstruction of lymphatic vessels in the mouse tail after cupping therapy

Running head: Cupping promotes lymphatic reconstruction

Fan-Wei Meng[1], Zhan-Ling Gao[1], Li Li[1], Lin-Lin Jie[1], Peng-Fei Yang[1], Zheng Liang[2], Ya-Wei Gao[3], Wen-Hui Liu[1]

[1]Department of Anatomy and Physiology, Shandong College of Traditional Chinese Medicine, Yantai, Shandong, China

[2]Biological Science and Technology Institute, Weifang Medical University, Weifang, China

[3]Department of Breast and Thyroid Surgery, Yantai Affiliated Hospital, Binzhou Medical University, Yantai, Shandong, China

Address for correspondence: Fan-Wei Meng, Department of Anatomy and Physiology, Shandong College of Traditional Chinese Medicine, No. 508 Binhaidonglu, Yantai 264199, Shandong, China, tel: +86 13853573075, fax: +86 05352765111, e-mail: 13853573075@163.com

Abstract

Background: To investigate the regulatory mechanism of local lymphatic reconstruction after cupping therapy in a mouse model.

Materials and methods: The lymphatic reconstruction process in the mouse tail after cupping therapy as well as the expression levels of the vascular endothelial identification molecule CD34, prospero homeobox protein 1 (PROX1), and lymphatic vessel endothelial hyaluronan receptor 1 (LYVE-1) were investigated for a duration of 4 days through immunohistochemistry experiments.

Results: On day 1 after cupping therapy, the $CD34^+$ and $LYVE\text{-}1^+$ cell densities were significantly increased, and the formed $CD34^+LYVE\text{-}1^+$ tubular structure started to express PROX1. This was followed by a decrease in both the $CD34^+$ and $LYVE\text{-}1^+$

stem cell densities to basal levels on the second day after cupping therapy. Both the $CD34^+$ and LYVE-1^+ cell densities subsequently increased again on the third day after cupping therapy. The increase in the LYVE-1^+ density was accompanied by tubular structure formation, which is characteristic of lymphangiogenesis. In addition, the colocalization of $CD34^+$ and LYVE-1^+ cells by immunohistochemistry suggests that the $CD34^+$ stem cells differentiated into new lymphatic endothelial cells.

Conclusions: Our findings indicate that the mechanism underlying the therapeutic effect of cupping therapy involves upregulation of vascular and lymphatic endothelial markers ($CD34^+$, LYVE-1^+, and $CD34^+$LYVE-1^+) in local tissues, which in turn promotes local new lymphatic vessel formation through the expression of PROX1.

Key words: Cupping; lymphatic regeneration; mice; LYVE-1; PROX1; CD34

INTRODUCTION

The lymphatic system was first discovered in 1627 by Gasparo Aselli [31]. Compared to the vasculature, the lymphatic system is an open system. The lymph from the peripheral lymphatic vessels in this system enters the lymph nodes, lymphatic trunks, and thoracic ducts [21], and the surrounding lymphatic vessel wall is connected to the surrounding tissue through filaments, a layer of overlapping endothelial cells. Due to the lack of a continuous basement membrane and tight junctions [3, 10, 15], filaments are the primary means of stabilization of the lymphatic vessel [11]. Under physiological conditions, most lymphatic vessels are collapsed. However, when the interstitial pressure increases, the filament “pulls” the lymphatic capillaries to ensure patency, promote drainage, and increase the lumen volume. The formation of new lymphatic vessels is an extremely important link between inflammation and the repair of damaged tissues [19].

Cupping therapy is a traditional form of alternative medicine for the prevention, treatment, and control of various diseases. It involves the application of suction through the adherence of glass or plastic cups to the skin. This therapy is believed to remove toxins, purge excess body heat, promote blood circulation, relieve swelling

and pain, dispel coldness, and activate the meridians, among other effects. Despite the gradual recognition and acceptance of cupping therapy, the physiological mechanism of how this therapy works is not yet clearly understood. Thus, this limits its widespread application. Clarification of the cupping mechanism is important not only for the development of the therapy itself, but also for the modernization, standardization, and globalization of traditional Chinese medicine. At present, the known therapeutic effects of cupping therapy include the purging of pus that had formed due to bacterial infection [4, 24, 27, 28] or a snake bite [32], stretching of muscles to increase the pain threshold [22], relieving fatigue [5], promoting blood circulation [8, 17], accelerating metabolism [12, 29, 30], modulating immune function [18], enhancing self-resistance [26], improving immunity [33], stimulating the nerves, and improving the general condition of the body [23, 25, 34]. The therapeutic effect primarily stems from the specific structural changes of the tissues as a result of the suction applied during cupping therapy. The application of a stimulus intensity of -0.04 MPa for 10 min during cupping has been reported to cause rupture of the capillaries and lead to ecchymosis [1]. The greater the suction force, the greater the rupture, and the deeper the color of the skin that had been cupped.

The morphological changes of the local lymph vessels after therapy and the mechanisms regulating the cupping process have not yet been elucidated. Therefore, the aim of this study was to investigate the expression profiles of the vascular endothelial identification molecule CD34, lymphatic vessel endothelial hyaluronan receptor 1 (LYVE-1), and its important regulatory molecule prospero homeobox protein 1 (PROX1) in the mouse tail after cupping therapy through immunohistochemistry experiments. The findings of this study will provide a theoretical basis for clinical treatment and lay the foundation for further related research.

MATERIALS AND METHODS

Materials

Specific pathogen-free Kunming mice, both males and female, weighing 18–26 g,

were provided by the Experimental Animal Center of Shandong University (Permit No.: SCXK (Lu) 20090001; Experimental animal license number: SYXK (Lu) 20100011). The goat anti-mouse LYVE-1 primary antibody was purchased from R&D Systems (Minneapolis, MN, USA). The donkey anti-rabbit and donkey anti-goat fluorescent secondary antibodies were purchased from Antgene Co. (Wuhan, China). The rabbit anti-mouse CD34 and rabbit anti-mouse PROX-1 primary antibodies, 0.01 M phosphate-buffered saline (pH 6.0), and the 3,3'-diaminobenzidine (DAB) immunostaining kit were purchased from Boster Biological Technology Co. (Wuhan, China). A DP-72 fluorescence microscope (Olympus, Japan) was used for the immunohistochemistry experiments.

Methods

Preparation of the mouse tail cupping model

Twenty 8-week-old mice, regardless of gender, were randomly divided into groups of four each: one control and four experimental groups (days 1, 2, 3, and 4 after negative-pressure application). After the mice in the experimental groups were anesthetized (50 mg/kg ketamine and 40 mg/kg benzylthiazine), all the mouse tails were placed in a vacuum suction device (7E-A) with negative-pressure application of 0.4 MPa for 15 min (to simulate cupping therapy), followed by the release of negative pressure. The tails of the control mice were placed in the same vacuum suction device without negative-pressure application. Handling of the experimental animals and the related manipulations were performed in accordance with the guidelines of the Ethics Committee of the Experimental Center of Shandong University of Traditional Chinese Medicine.

Immunohistochemistry

Hematoxylin and eosin (H&E) staining

At 1 to 4 days after cupping therapy, a 4-μm tail section from one mouse from each experimental group was prepared through conventional fixation with 40 g/L formaldehyde, followed by decalcification with EDTA and paraffin embedding. H&E

staining was then performed to observe the expression patterns of LYVE-1, CD34, and PROX1 in the tissue sections of the mouse tail using a DP-72 fluorescence microscope (Olympus, Japan).

Double fluorescence staining

Tissue sections were deparaffinized and immunostained. After inactivating endogenous peroxidase with 0.3% (v/v) hydrogen peroxide solution, the tissue sections were incubated with primary antibodies against PROX1 (rabbit anti-mouse antibody; 1:200), CD34 (1:100), and LYVE-1 (goat anti-mouse antibody; 1:100; Boster Co., Wuhan, China) at 4 °C for 24 h. This was followed by incubation with the secondary antibody horseradish peroxidase-labeled goat anti-rabbit IgG or rabbit anti-goat IgG (Boster Co., Wuhan, China), before adding the DAB substrate (Wuhan, China) for visualization with a DP-72 light microscope. Each slice was imaged 50 times at 400× magnification. Semi-quantitative analysis was performed using Image-Pro Plus 6.0 software, and the average area was calculated. Next, the immunofluorescence-stained tissue sections were subjected to another round of immunostaining through incubation with rabbit anti-mouse PROX1 (1:100) and goat anti-mouse LYVE-1 (1:100) primary antibodies, followed by the simultaneous addition of rabbit anti-mouse CD34 (1:100) and goat anti-mouse LYVE-1 (1:100) at 4 °C for 24 h. Subsequent incubation with either Cy3-labeled donkey anti-goat IgG or FITC-labeled donkey anti-rabbit IgG secondary antibodies was performed, and the sections were visualized using a DP-72 fluorescence microscope (Olympus, Japan).

Statistical analysis

Statistical analysis was performed using SPSS version 16.0 (Chicago, IL, USA), and Microsoft Excel was used for data presentation. Data from four mouse tails in each group were expressed as the mean ± standard deviation (SD). Comparison between two groups was performed using the T-test, and comparisons among three or more groups were performed using one-way analysis of variance followed by Fisher's least significant difference test. A p value < 0.05 was considered statistically

significant.

RESULTS

Negative pressure application does not affect subcutaneous tissue integrity

The subcutaneous structure of loose connective tissue in the control group appeared well-defined with a regular distribution of the arteries, veins, nerves, loose fibers, normal axons, and adventitial spaces (Fig. 1A). H&E staining revealed that there was no significant change in the number of blood vessels or nerves in the subcutaneous tissue of the mouse tail at 1 to 4 days after negative-pressure application (Fig. 1B–E; $p>0.05$). After cupping, the body mass, tail temperature, and blood flow returned to normal levels ($p>0.05$).

Effect of cupping therapy on the cellular distribution of LYVE-1$^+$ and CD34$^+$

The vascular endothelial cell marker molecule CD34$^+$ and LYVE-1$^+$, which are characteristic of blood vessels and lymphatic vessels, respectively, regulate the regeneration of lymphatic endothelial cells. The CD34$^+$ marker can be observed in vascular endothelial cells as well as in hematopoietic stem cells. We observed CD34$^+$ (red) and LYVE-1$^+$ (green) tubular structures in the perivasculature of subcutaneous, epimyocardial, and tubular tissues in the control group (Fig. 2A). At 1 day after cupping therapy, the numbers of CD34$^+$ and LYVE-1$^+$ cells were significantly increased (Fig. 3), showing a spot-like distribution (Fig. 2B). However, at 2 days after cupping therapy, the average areas of both LYVE-1$^+$ (Fig. 3A) and CD34$^+$ (Fig. 3B) cells decreased to basal levels comparable with that of the control group. This was followed by an increase in their average areas on day 3 after cupping treatment, wherein an approximately 2-fold increase in the LYVE-1$^+$ density was observed (Fig. 3A; $p\leq0.05$), and the cells formed a tubular structure with an expanded lumen. Unlike the high LYVE-1$^+$ density on day 4 after cupping treatment, the CD34$^+$ density dropped back to basal levels (Fig. 3B).

Cupping promotes LYVE-1 and PROX1 expression

Next, the expression of another lymphatic endothelial cell marker, PROX1, was investigated. LYVE-1 (green) and PROX1 (red) were observed to colocalize in the lymphatic vessels (yellow) at 1 day after cupping therapy (Fig. 4). This result suggests that cupping promotes lymphangiogenesis. Similarly, LYVE-1 was observed to colocalize (yellow) with CD34 (red) at 1 day after cupping therapy (Fig. 5). $CD34^+LYVE\text{-}1^+$ expression can function as a hematopoietic stem cell marker of blood vessels and as an intermediate-stage stem cell marker during the differentiation of lymphatic endothelial cells [9, 14]. Taken together, these findings indicate that cupping induces $CD34^+LYVE\text{-}1^+$ stem cells to initiate lymphangiogenesis.

DISCUSSION

A literature search performed before conducting this study yielded no relevant reports of cupping research using animal models. Hence, we designed this study to examine the morphological effects of cupping treatment in the mouse tail. We used a negative-pressure cupping device to apply a negative pressure of 0.04 MPa for 15 min to simulate cupping. The expression of CD34, a marker of endothelial progenitor cells and newborn capillary endothelial cells [13, 16]; LYVE-1, a lymphatic endothelial cell-specific marker [2, 7]; and PROX1, a marker for the differentiation of endothelial progenitor cells into lymphatic endothelial cells [6, 20]; were examined in this study using immunohistochemistry to investigate the reconstruction of blood vessels and lymphatic vessels after the cupping treatment. Of note, we observed an increased $CD34^+$ cell density but not angiogenesis. In contrast, tubular structure formation (lymphatic vessel) and a 2-fold increase in the number of $LYVE\text{-}1^+$ cells were observed after cupping therapy. Thus, we conclude that there is obvious lymphangiogenesis but not new blood vessel formation after cupping therapy and that an increased number of $CD34^+$ cells induces differentiation into lymphatic endothelial cells.

The number of $CD34^+$ and $LYVE\text{-}1^+$ cells in the local tissue increased significantly at 1 day after the cupping treatment due to the formation of a $CD34^+LYVE\text{-}1^+$ tubular structure. In addition, PROX1 expression was observed in the lymphatic endothelial cells at 1 day after cupping therapy. The decrease in the

number of LYVE-1$^+$ cells at 2 days after cupping therapy is likely because of lymphatic vessel rupture, which causes LYVE-1$^+$ necrosis. Since lymphatic vessels have thinner walls than arteries and veins, they are more susceptible to rupture under the same negative-pressure stimulus. The increase in LYVE-1$^+$ cells due to the formation of new lymphatic vessels at 3 and 4 days after cupping therapy suggests that lymphatic reconstruction is an active process. A similar trend was observed for the CD34$^+$ cells during the first 3 days after cupping therapy, wherein an initial increase in the average area of CD34$^+$ cells was noted on day 1 after cupping treatment. However, on day 2 after cupping, the CD34$^+$ cell density decreased to basal levels, indicating that no new blood vessels had formed. This finding suggests that CD34$^+$ cells are probably sensitive to negative-pressure stimulation. Unlike LYVE-1$^+$ cells, the average CD34$^+$ density did not significantly increase on days 3 and 4 after cupping therapy, suggesting that blood capillaries are sufficiently strong to withstand negative-pressure stimulation so neovascularization was not obvious.

Three important conclusions can be drawn from this experiment. Firstly, cupping therapy involving controlled negative-pressure application can increase the number of local vascular endothelial stem cells (CD34$^+$) and lymphatic endothelial stem cells (LYVE-1$^+$). Secondly, PROX1, a key gene for the regeneration of lymphatic endothelial cells, can be activated to regulate the reconstruction of local lymphatic vessels. Lastly, the upregulation of PROX1, LYVE-1, and CD34 does not lead to significant neovascularization but leads to lymphangiogenesis instead. Therefore, we speculate that the mechanism of cupping may be achieved by first activating the pluripotent stem cells in the local tissues, followed by reconstruction of the local lymphatic network instead of the neovascular network to repair damaged tissue cells, thereby increasing tissue renewal. Moreover, we demonstrated for the first time that the mouse tail can be used to study the mechanism of cupping. The ease of handling of mice and the good reproducibility of the results from our study support the use of mice as a good animal model for future related research.

The limitations of cupping therapy research include the challenge in performing operations on fur-covered animals, the lack of suitable animal models, and the

difficulty in controlling the suction force applied during cupping therapy, among others. Only one negative-pressure value (0.04 MPa) and fixed duration of pressure application (15 min) was tested in this study. Since blood vessels have a higher pressure tolerance than lymphatic vessels, using a higher negative-pressure stimulus can cause blood vessel rupture and thereby stimulate angiogenesis. In the future, the focus should be on elucidating the effect of varying the amount of negative pressure applied and the duration of the pressure application. Also, the signal transduction pathway for negative pressure should be further investigated. Our findings propose lymphangiogenesis-induced blood recirculation as the underlying mechanism of the therapeutic effect of cupping, thus providing greater support for its clinical application in pain relief.

Acknowledgments

We would like to acknowledge *Medjaden* Bioscience Limited for editing and proofreading this manuscript.

Funding sources

This study was supported by the Administration of Traditional Chinese Medicine of Shandong Province (No. 2017-147).

Conflicts of interest

The authors declare that they have no conflicts of interest.

References

1. Asellius G. De lactibussivelacteisvenis. JB Bidellium, Milan. 1627.
2. Banerji S, Ni J, Wang SX, et al. LYVE-1, a new homologue of the CD44 glycoprotein, is a lymph-specific receptor for hyaluronan. J Cell Biol. 1999; 144:789-801.
3. Barsky SH, Baker A, Siegal GP, et al. Use of anti-basement membrane antibodies

to distinguish blood vessel capillaries from lymphatic capillaries. Am J Surg Pathol. 1983; 7:667-677.

4. Dong XJ, Li YJ, Zhang CY. Application of cupping therapy in the treatment of chronic osteomyelitis. Chinese Journal of Traditional Chinese Medicine and Traumatology. 2006; 14:26-27.
5. Farhadi K, Schwebel DC, Saeb M, et al. The effectiveness of wet-cupping for nonspecific low back pain in Iran: a randomized controlled trial. Complement Ther Med. 2009; 17:9-15.
6. Hong YK, Harvey N, Noh YH, et al. Prox1 is a master control gene in the program specifying lymphatic endothelial cell fate. Dev Dyn. 2002; 225:351-357.
7. Jackson DG, Prevo R, Clasper S, et al. LYVE-1, the lymphatic system and tumor lymphangiogenesis. Trends Immunol. 2001; 22:317-321.
8. Jin L, Liu YY, Meng XW. The initial observation of the influence of cupping on the blood flow of healthy human back skin. Acupuncture and Moxibustion Clinical Journal. 2010; 26:4-5.
9. Kriehuber E, Breiteneder-Geleff S, Groeger M, et al. Isolation and characterization of dermal lymphatic and blood endothelial cells reveal stable and functionally specialized cell lineages. J Exp Med. 2001; 194:797-808.
10. Leak LV, Burke JF. Electron microscopic study of lymphatic capillaries in the removal of connective tissue fluids and particulate substances. Lymphology. 1968; 1:39-52.
11. Leak LV, Burke JF. Fine structure of the lymphatic capillary and the adjoining connective tissue area. Am J Anat. 1966; 118:785-809.
12. Li CQ, Meng XW, Y. G. Views of Temperature Changes of Duke Point in Healthy Adults Before and After Cupping with Dazhui The 9th National Acupuncture and MoxibustionTuina Symposium of the Chinese Acupuncture and Moxibustion Society Beijing: Chinese Acupuncture Society. 2010:92-94.
13. Peichev M, Naiyer AJ, Pereira D, et al. Expression of VEGFR-2 and AC133 by circulating human CD34(+) cells identifies a population of functional endothelial

precursors. Blood. 2000; 95:952-958.

14. Salven P, Mustjoki S, Alitalo R, et al. VEGFR-3 and CD133 identify a population of CD34+ lymphatic/vascular endothelial precursor cells. Blood. 2003; 101:168-172.
15. Sauter B, Foedinger D, Sterniczky B, et al. Immunoelectron microscopic characterization of human dermal lymphatic microvascular endothelial cells. Differential expression of CD31, CD34, and type IV collagen with lymphatic endothelial cells vs blood capillary endothelial cells in normal human skin, lymphangioma, and hemangioma in situ. J Histochem Cytochem. 1998; 46:165-176.
16. Shintani S, Murohara T, Ikeda H, et al. Mobilization of endothelial progenitor cells in patients with acute myocardial infarction. Circulation. 2001; 103:2776-2779.
17. Tian YX, Qin LN, Zhang WB. Initial observation of the effect of different cupping negative pressure on skin blood flow. Acupuncture Research. 2007; 32:184-185.
18. Wang HS, Fu WX. The effect of canning on the elimination of urea nitrogen, uric acid and creatinine caused by exercise fatigue in rats. Shaanxi, Chinese Medicine. 2000; 21:575.
19. Watari K, Nakao S, Fotovati A, et al. Role of macrophages in inflammatory lymphangiogenesis: Enhanced production of vascular endothelial growth factor C and D through NF-kappaB activation. Biochem Biophys Res Commun. 2008; 377:826-831.
20. Wigle JT, Oliver G. Prox1 function is required for the development of the murine lymphatic system. Cell. 1999; 98:769-778.
21. Witte MH, Bernas MJ, Martin CP, et al. Lymphangiogenesis and lymphangiodysplasia: from molecular to clinical lymphology. Microsc Res Tech. 2001; 55:122-145.
22. Xin Y, Wang SP, Fang XF. Pain threshold and skin temperature observation before and after single cupping. Chinese Journal of Physical Therapy. 1994;

17:173-174.

23. Xu YY. Walking cans for the treatment of irritable bowel syndrome in 48 cases. Zhejiang Journal of Traditional Chinese Medicine. 2007; 42:163.

24. Yang WL, Dong ZC, Zhang JL. Application of Cupping in the Treatment of Sputum Syndrome. Journal of Shaanxi College of Traditional Chinese Medicine. 2004; 27:44-45.

25. Yao X. Follow-up cupping with acupuncture treatment of chronic diarrhea efficacy observation. Jilin Medical. 2006; 27:1403-1404.

26. Ye LH. The effect of health cupping on human immune function. Modern Rehabilitation. 1998; 23:1109-1121.

27. Yu XJ. Experience of Cupping Therapy for Bleeding Treatment. Journal of Traditional Chinese Medicine. 2010; s2:239-240.

28. Zha BG, Wang ZY. Cupping method for the promotion of foot infection wound healing in 28 cases. Hunan Journal of Traditional Chinese Medicine. 2005; 21:81.

29. Zhang L. Cupping therapy on the skin temperature and hemoglobin effects. Beijing: Beijing University of Chinese Medicine. 2000.

30. Zhang L, Tang LT, Tong XL. The effect of cupping therapy on human local hemoglobin and its analysis. Chinese Acupuncture and Moxibustion. 2001; 21:619-621.

31. Zhao XX, Tong BJ, Wang XX. Initial observation of the influence of time and pressure on the color of cupping jars. Chinese Acupuncture and Moxibustion. 2009; 29:385-388.

32. Zhong JR, Zhao YH, Liang QS. Early applications and the like. Cupping instrument snake bites in contemporary Chinese Medicine. 2010; 17:19-21.

33. Zhong L, Li L, Li J. Walking cans on the immune function of red blood cells. Chinese Acupuncture. 1999; 19:367-368.

34. Zhou Y, Wu RM, Cao Y. Cupping treatment of patients with pneumonia and nursing experience. Journal of Guiyang College of Traditional Chinese Medicine. 2010; 32:54-55.

FIGURE LEGENDS

Figure 1. H&E staining of mouse tails for the (A) control group and (B–E) the experimental groups at 1–4 days after cupping therapy, respectively, at 400× magnification. Compared with the control group, there was no significant change in the morphology or the number of blood vessels (→) or nerves ( ) in the subcutaneous tissue of mouse tails after cupping therapy.

Figure 2. Double fluorescence staining images showing the expression of LYVE-1 (green) and CD34 (red) in mouse tails in (A) the control group and (B–E) the experimental groups at 1–4 days after cupping therapy, respectively. Compared with the control group, the numbers of $CD34^+$ and $LYVE\text{-}1^+$ cells increased significantly (B) at 1 day after cupping therapy. (C–E) During the next 2 to 4 days, the number of $CD34^+$ vessels gradually decreased, and the number of $LYVE\text{-}1^+$ lymphatic vessels continued to increase.

Figure 3. Plots showing the effect on the average cell densities of (A) $LYVE\text{-}1^+$ and (B) $CD34^+$ in the mouse tail after cupping therapy. * denotes $p \leq 0.05$.

Figure 4. Double fluorescence staining images at 400× magnification showing the expression of (A) LYVE-1 (green; spot-like structures), (B) PROX1 (red; observed as tubular structures), and (C) their merged images (yellow indicates differentiation into new lymphatic endothelial cells) in a mouse tail at 1 day after cupping therapy.

Figure 5. Double fluorescence staining images (400× magnification) showing the expression of (A) LYVE-1 (green), (B) CD34 (red), and (C) their merged (yellow) images of the rear portion of a mouse tail at 1 day after cupping therapy. $LYVE\text{-}1^+CD34^+$ tubular structures appear more obvious after cupping treatment.


A
B
C
D
E

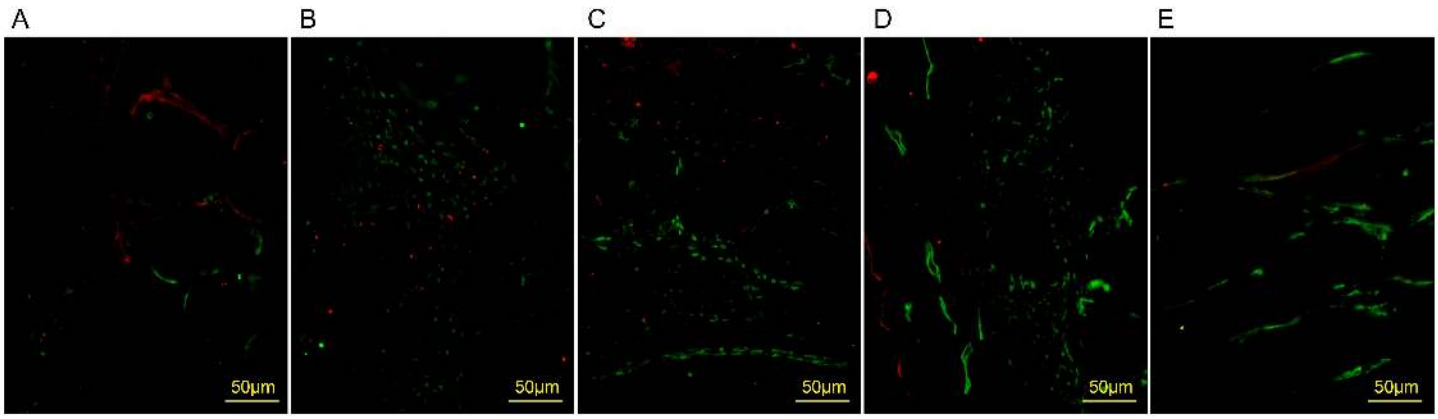
A
B
C
D
E
50μm
50μm
50μm
50μm
50μm

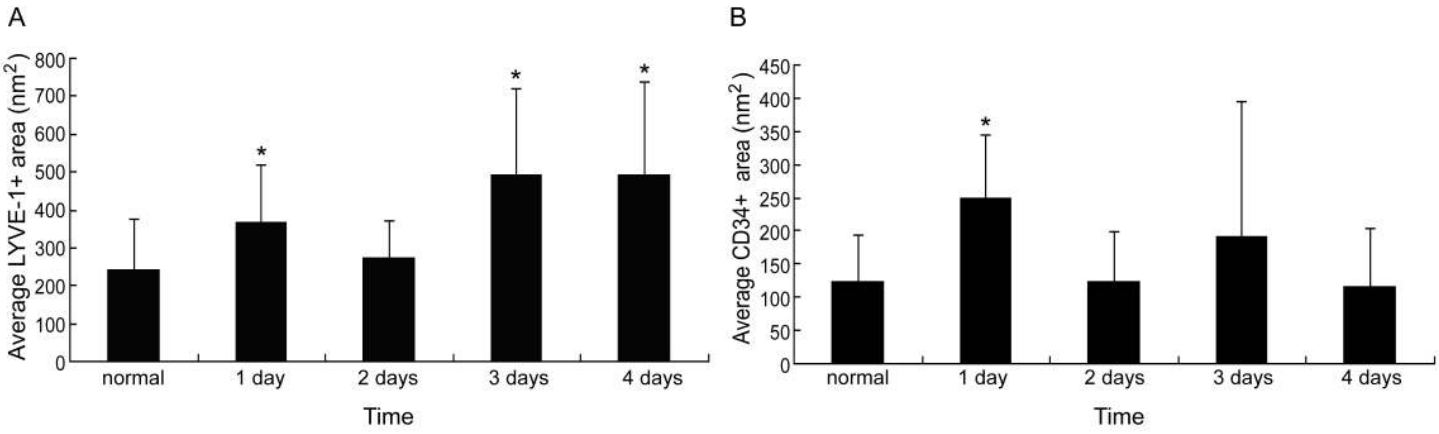
A
Average LYVE-1+ area (nm2)
800
700
600
500
400
300
200
100
0
*
*
*
normal
1 day
2 days
3 days
4 days
Time
B
Average CD34+ area (nm2)
450
400
350
300
250
200
150
100
50
0
*
normal
1 day
2 days
3 days
4 days
Time

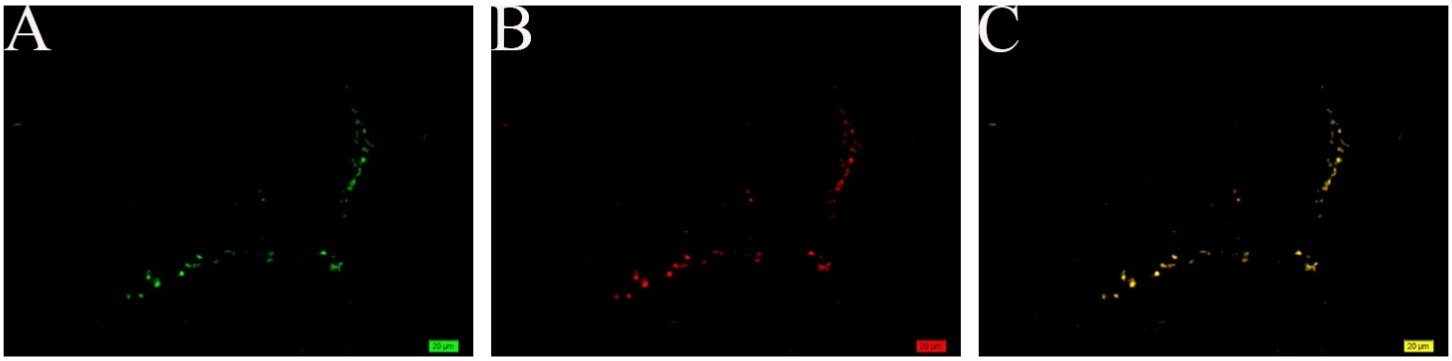
A
B
C
20 μm
20 μm
20 μm

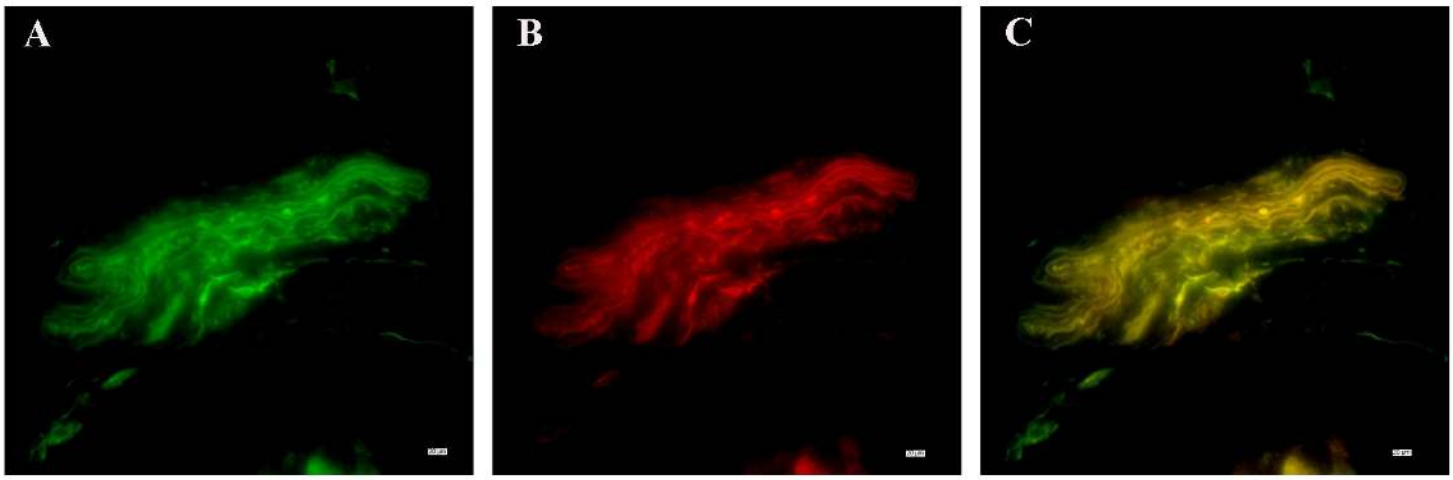
A
B
C